APPLICATION OF RECEIVER FUNCTION TECHNIQUE TO WESTERN TURKEY

Timur TEZEL[*] **Supervisor: Takuo SHIBUTANI**[**]
MEE07169

ABSTRACT

In this study I tried to determine the shear wave velocity structure in the crust and uppermost upper mantle using receiver function technique. For this purpose I selected teleseismic earthquakes in the epicentral distances between 30 and 90 degrees, magnitudes of which are greater than 6.3. I collected waveform data recorded at Turkey's broadband seismic stations between 2006 and 2008. I used radial receiver functions which were calculated using extended time multitaper method to determine the crustal and uppermost upper mantle structure. My study consists of three steps: receiver function (RF) calculation, RF image and RF inversion. Because of the data availability, I studied data of 33 stations in western Turkey which belong to the General Directorate of Disaster Affairs Earthquake Research Department and Bogazici University Kandilli Observatory. First, I calculated radial receiver functions for each station. In the next step, I made two RF images using the RFs from stations along two lines: the one is running from the northeast of Bozcaada to Konya city and the other is running from the north of Izmir to the northeast corner of Rhodes island. In the third step, I applied genetic algorithm inversion method to determine the shear wave velocity structure beneath six seismic stations.

The results show that the Moho depth changes from region to region; we observed that the Moho depth is around 35 km and 25 km beneath the former and latter profiles, respectively. The results of receiver function inversion are consistent with these RF images. Shear wave velocities were estimated to be in the range between 3.5 and 3.9 km/s for the lower crust and between 4.0 and 4.6 km/s for the uppermost upper mantle, respectively.

Keywords: Receiver Function, Crust, Teleseismic Wave, Turkey.

INTRODUCTION

Turkey has experienced many natural disasters which have caused serious casualty, collapse of buildings, economical losses up to now. Among these disasters, earthquakes are the first to be concerned rather than land slides, floods, rock falls, avalanches, and droughts. In Turkey, earthquakes occur in the upper crust generally, and one of the important issues is to determine discontinuities and velocity changes in the crust and also to determine the transition to the Moho. There are some seismological studies to find a velocity model using travel time tomography, surface wave group velocity inversion, reflection profiling, and receiver function method etc. Determination of the discontinuities and especially shear wave velocity structure has an important role in the planning of the urban areas and cities. In this study, we applied receiver function method to determination of shear wave velocity structures beneath the seismic stations in Turkey.

[*]General Directorate of Disaster Affairs Earthquake Research Department, Ankara, Turkey.
[**]Assoc. Professor, Disaster Prevention Center, Research Center of Earthquake Prediction, Kyoto University, Japan.

DATA

I used teleseismic waveform data for 50 earthquakes recorded by General Directorate of Disaster Affairs Earthquake Research Department (here after ERD) and Boğaziçi University Kandilli Observatory (KOERI) broadband stations. I selected 33 broadband stations which are located in western Turkey. Selection criteria were as follows: magnitude of earthquakes should be greater than 6.3 and epicentral distance should be between 30˚ and 90˚.

Data were obtained from KOERI via internet (http://barbar.koeri.boun.edu.tr) and from ERD via CD-R.

THEORY AND METHODOLOGY

The Receiver Function technique is used for determination of crustal structure beneath seismic stations. Teleseismic records ($30^\circ \leq \Delta \leq 90^\circ$) are used in this method. Teleseismic P waveforms contain information related to source, propagation path and local structure beneath the recording station. The method uses the coda part of the P wave which includes converted phases and reverberations generated at discontinuities beneath each station and convolved with source function and instrumental impulse responses. If we eliminate the source and instrumental effects from waveforms, they provide information about the local velocity structure under the seismic station. In Figure 1, we can see the simple ray diagram for the incident wave and its converted and reverberated phases.

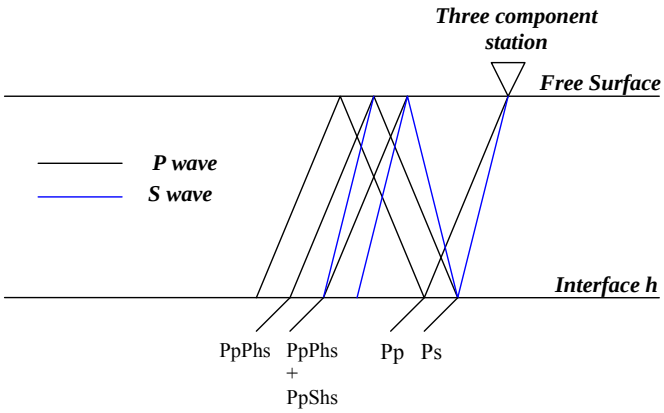

Figure 1. Simplified ray diagram identifying the major P to S converted phases which comprise the receiver function for a single layer over a half-space under the seismic station (modified from Ammon(1990)).

A teleseismic P wave arrives at the recording station with both a constant and relatively large horizontal phase velocity (15-25 km/s). This phase velocity justifies a plane wave and simplifies the study of the resulting ground motion (Ammon, 1990).

Receiver Function Calculation

Determination of the velocity structure of the crust and upper mantle beneath a single seismic station can be done by using teleseismic receiver functions. The receiver function analysis uses the converted phases and multiples recorded on the horizontal seismograms (e.g. Burdick and Langston, 1977; Langston 1977, 1979; Owens *et al*., 1984; Ammon, 1991).

$$
\begin{aligned}
D_V(t) &= I(t) * S(t) * E_V(t) \\
D_R(t) &= I(t) * S(t) * E_R(t) \\
D_T(t) &= I(t) * S(t) * E_T(t)
\end{aligned} \tag{1}
$$

Here, *V, R, T* shows vertical, radial and tangential components respectively. Also, *I(t)* is impulse response of the recording instrument, *S(t)* is the seismic source function, $E_V(t)$, $E_R(t)$, $E_T(t)$ are the vertical, radial and tangential impulse response of the earth structure. And asterisk (*) shows the convolution operator.

As earth structure beneath a station will produce phase conversions of the P to S type, horizontal components of ground motion will be different from the vertical component. $D_V(t)$ contains the factors which we wish to remove from observed seismograms, so isolating $E_R(t)$ and $E_T(t)$ can be accomplished by deconvolving $D_V(t)$ from $D_R(t)$ and $D_T(t)$. In receiver function method, there are several stabilization methods; they are the water level method, the multitaper method, the extended time multitaper method. In this study I used the extended time multitaper method which was improved by Shibutani *et al*. (2008) based on Park and Levin (2000) and Helffrich (2006). In this method, they used the three lowest-order 4π prolate eigentapers of 50 sec duration. They summed the multitapers with 75 % window overlap. The multitapers smoothly are connected at the junctions, and the resultant taper has a flat level. If we use the flat part for windowing the P onset and the P coda, we can estimate the relative amplitudes of receiver functions (Shibutani *et al*., 2008). As a result, the frequency-domain receiver function is defined by

$$
E_R(\omega) = \frac{\sum_{k=0}^{K-1} H^{(k)}(\omega)\tilde{U}^k(\omega)}{\sum_{k=0}^{K-1} U^{(k)}(\omega)\tilde{U}^{(k)}(\omega) + \left(\frac{J_S}{J_N}\right)^2 \sum_{k=0}^{K-1} N^{(k)}(\omega)\tilde{N}^k(\omega)} G(\omega) \tag{2}
$$

where $H^{(k)}(\omega)$ and $U^{(k)}(\omega)$ denotes the Fourier spectrum of the radial or transverse and vertical components of the waveform data with the kth prolate eigentaper, and $N^{(k)}(\omega)$ is the Fourier spectrum of presignal noise of the vertical component waveform. J_S and J_N are the numbers of the multitapers used for the signal and presignal. The second term in the right-hand side of equation (2) is a Gaussian high cut filter in which *a* controls the the corner frequency. In this study, I set *a* to 2, and then the corner frequency becomes 0.3 Hz. I showed calculated radial receiver functions with this method for two stations (GDZ and KDHN) in Fig. 2. In these figures, we can see the difference between waveforms of receiver functions related with backazimuth. It reflects the complexity beneath the stations and the lateral change of earth structure.

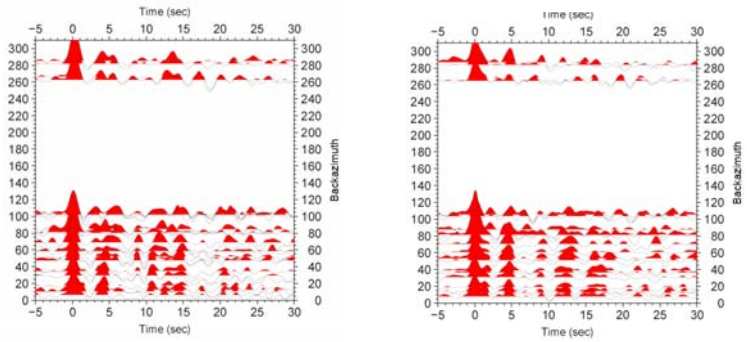

Figure 2. Calculated receiver functions for the GDZ and KDHN stations are shown on the left and right panel, respectively. Receiver functions are ordered by backazimuth and positive amplitudes are colored by red.

Receiver Function Image

The peaks and troughs of receiver functions correspond to boundaries of the S-wave velocity structure, and the time axis of the receiver functions can be converted to the depth axis using a 1-D velocity model. Delay time between converted Ps phase and direct Pp phase is given by the below equation,

$$T_{ps}(Z) = \int_{z=0}^{z=Z} \left(\sqrt{\frac{1}{\beta(z)^2} - p^2} - \sqrt{\frac{1}{\alpha(z)^2} - p^2} \right) dz \qquad (3)$$

where α and β are P and S wave velocities as a function of depth z respectively, Z indicates the depth of the interfaces, and p is the ray parameter. The converted receiver functions can be represented by a bending ray with the ray parameter and a backazimuth. I projected the rays into 1 km by 1 km cells. I used four 1-D velocity models: the three models W1, W2, and W3 are based on Tezel *et al*. (2007) and the fourth model is AK135 (Kennett *et al*. 1995). Figure 3 shows the 1-D velocity models (W1, W2, W3 and AK135) and two lines: the one is running from the northeast of Bozcaada to Konya city and the other is running from the north of Izmir to the northeast corner of Rhodes island along which RF images are processed. Figure 4 shows the images obtained by this method. In the figures, the positive amplitudes of the receiver functions are indicated by the red color and indicate velocity discontinuities at the top of high velocity layers. In Figure 4, 2-D RF images reflect the relation between earth structure and 1-D velocity models W1, W2, W3 and AK135 respectively.

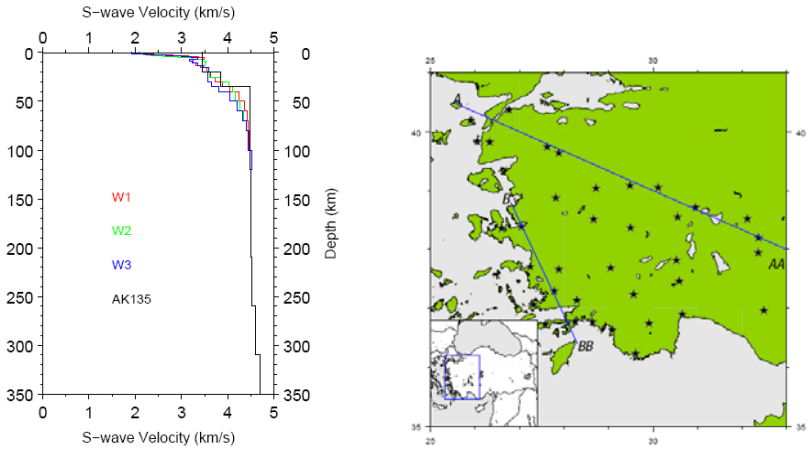

Figure 3. Input 1-D velocity models based on Tezel *et al.* (2007) and Kennett *et al.* (1995) and selected image lines (A-AA and B-BB).

Receiver Function Inversion

In previous studies, a linearization procedure was used to invert the receiver function which requires the initial model to be close to the true velocity structure. Ammon (1990) showed that the final models were dependent on the initial models. For this reason in this study I used the genetic algorithm (GA) (Shibutani *et al*. 1996).

In this study, I applied this inversion technique to radial receiver functions of the six broadband stations. For this purpose radial receiver functions were stacked according to the backazimuths and RF waveform similarities for each station. I tried to model the crust and uppermost mantle down to 50 km with six major layers: a sediment layer, basement layer, upper crust, middle crust, lower crust and uppermost mantle. The model parameters in each layer are the thickness, the S wave velocity. The velocity ratio between P and S waves (Vp/Vs) and the density in the sediment and basement layers are also model parameters. For each model parameter, upper and lower bounds and 2^n

possible values are specified. The size of the model space to be searched is $2^{46} \approx 7.04 \times 10^{13}$. Figure 5 shows the Moho depth estimated for these stations.

DISCUSSIONS AND CONCLUSIONS

In this study I applied RF (receiver function) technique to determine the velocity discontinuities such as Moho etc. Moreover, I applied genetic algorithm using receiver functions to determine the shear wave velocity structure beneath six seismic stations. I used only radial receiver functions (I calculated the tangential receiver functions but not used them in the interpretation). After calculation of receiver functions, I employed 2-D image technique which converts the time axis to depth axis using 1-D velocity models and shows the amplitudes with colors. Red (blue) color shows positive (negative) amplitude which indicates the increase (decrease) in the velocity. Along A-AA and B-BB lines I applied this method and some velocity discontinuities were detected and indicated by red dotted lines (Fig. 4).

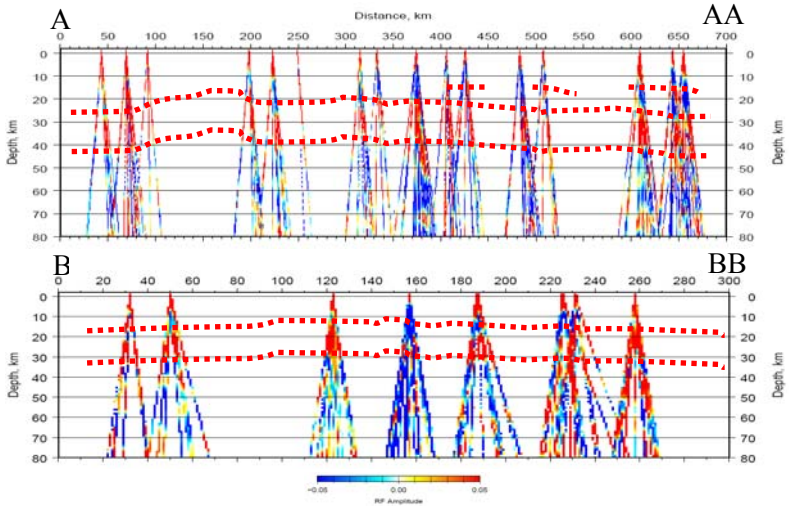

Figure 4. RF images for the A-AA and B-BB lines using W3 1-D velocity model.

We interpreted that Moho should lie between 30 and 40 km for line A-AA and probably around 35 km. For some stations we can see another signature around the 15 km, which was interpreted as Conrad discontinuity. In line B-BB Moho discontinuity seems placed between 20 and 30 km depth and probably around 25 km.

After RF image process I employed the genetic algorithm to determine the shear wave velocity model beneath seismic stations. I selected six broadband stations (BALB, GDZ, ALT, KDHN, LADK, KONT) that have more data and show good RF results. I stacked the RFs according to the backazimuths and then applied inversion process for each station.

Synthetic receiver functions generally show good fitting with the observed waveforms. Shear wave velocity models which were derived from inversion indicate that general character of crust – mantle boundary in the region. The depth of the boundary for each station was determined. Shear wave velocities near the surface varied between 1.5 and 3.5 km/s and at the mid – crustal depth range between 3 and 4 km/s. Sub Moho velocities are between 4 and 4.6 km/s. The results for some groups (made based on backazimuths) for the stations KONT, ALT and GDZ indicate low velocity zone between 25 and 35 km.

Figure 5 show the estimated Moho depths for six stations. These velocity values are generally similar to those of previous studies, while we can not observe low velocity layer around 10 km that was mentioned by previous studies.

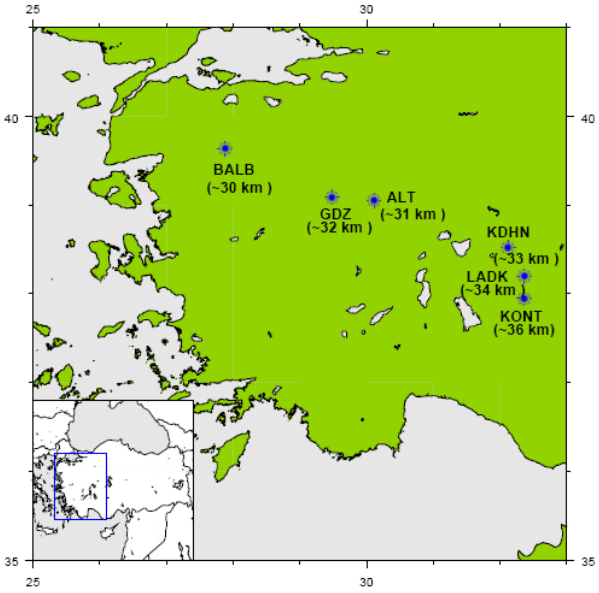

Figure 5. Moho depths calculated from inverison

Results of this study with RF image and RF inversion show the Moho thinner in the west of study area than in the east part. These results similar to the previous studies which were mentioned the Moho depth changes from 30 km to 38 km from the west to the east of Turkey. Moreover, other stations which were used for the receiver function show complex receiver waveforms, which reflect the complex tectonic structure around the study area. Also, difference between A-AA and B-BB profiles suggest that the study area is not a homogenous area and that deformation is different in each area. In these RF images Moho discontinuity has been seen as a wide band caused by the Gaussian filter used the mean value for the Moho depth considering the error range (i.e. ± 5 km). This study is a preliminary attempt to determine the Moho discontinuity based on RF image and will contribute to construction of a reliable reference velocity model in Turkey.

AKNOWLEDGEMENT

I would like to express my sincere gratitude to my adviser Dr. T. Hara for his suggestions and contributions to my study.

REFERENCES

Ammon, C.J., 1990, J. Geophy. Res., 95, 15303-15318.
Ammon, C.J., 1991, Bull. Seism. Soc. Am., 81, 2504-2510.
Burdick, L.J., and Langston, A.C., 1977, Bull. Seism. Soc. Am., 67, 677-691.
Helffrich, G., 2006, Bull. Seism. Soc. Am., 96, 344-347.
Kennett B.L.N., Engdahl E.R., and Buland, R., 1995, Geophys. J. Int., 122, 108-124.
Langston, C.A., 1977, Bull. Seism. Soc. Am., 67, 1029-1050.
Langston, C. A., 1979, J.Geophys.Res., 84, 4749-4762.
Owens, T. J., Zandt, G., and Taylor, S.R., 1984, J.Geophys. Res., 89, 7783-7795.
Park, J., and Levin, V., 2000, Bull. Seismo. Soc. Am., 90, 1517-1520.
Shibutani, T., Sambridge, M., and Kennett, B., 1996, Geophy. Res. Let., 23, 1829-1832.
Shibutani, T., Ueno, T., and Hirahara, K., 2008, Bull. Seismo. Soc. Am., 98, 812-816.
Tezel, T., Erduran, M., and Alptekin, Ö., 2007, Annals of Geophysics, Vol.50, No.2, pp. 177-190.